

## **TEXTURE DEVELOPMENT IN Al-2.3%Li**

O. ENGLER, K. LÜCKE

Institut für Metallkunde und Metallphysik  
RWTH Aachen, D-5100 Aachen, West Germany

### **ABSTRACT**

The texture development in Al-2.3%Li during cold rolling, cross rolling and subsequent recrystallization annealing is investigated by means of X-ray pole figures and ODF analysis. The results are discussed in terms of Taylor-type deformation models and of nucleation and growth models for recrystallization.

### **INTRODUCTION**

One of the main problems of the new generation Al-Li alloys which still prohibits their technical use is their marked anisotropic mechanical behaviour. It is well known by now, that this anisotropy is caused by pronounced textures<sup>1</sup>. In earlier papers by the present authors<sup>2,3</sup> it was shown that the cold rolling texture development of the commercial Al-Li alloy 8090 is strongly influenced by the starting texture as well as by the precipitation state, as had also been found for conventional Al-alloys<sup>4-6</sup>. During recrystallization the texture sharpness decreases thus giving rise to better mechanical properties, but detailed investigations of these texture changes are completely missing yet.

As the deformation and the recrystallization behaviour of commercial Al-Li alloys is very complex due to the various alloying elements, in the present study the influence of Li on the rolling and recrystallization texture development was investigated for a high purity binary Al-2.3%wt Li alloy.

### **RESULTS OF DEFORMATION EXPERIMENTS**

After appropriate pre-treatment a homogeneous structure with equiaxed grains (~200µm) exhibiting a rather random starting texture (see below) was achieved. One specimen of this material was homogeneously cold rolled to reductions from 50% to 97.5%, another one was cross rolled by changing the rolling direction by 90° after each rolling step of ~10%. In order to analyse the obtained textures, besides pole figures the ghost corrected Orientation Distribution Functions (ODFs) were calculated from four pole figures (for details see e.g. 4). As an example Fig. 1a,b exhibits the {111}-pole figures and Fig. 2a,b the ODFs for the two samples deformed by 90%.

The straight rolled sample reveals a typical fcc rolling texture with most orientations assembled along the  $\beta$ -fibre running from C- $\langle 112 \rangle \langle 111 \rangle$  over S- $\langle 123 \rangle \langle 634 \rangle$  to B- $\langle 011 \rangle \langle 211 \rangle$ . Such textures can very comprehensively be described by plotting the orientation density along this fibre versus  $\varphi_2$  as shown in Fig.3a for various degrees of rolling. The curves for the starting material (0%, filled symbols) exhibit a rather random texture. During rolling the samples develop a typical Al rolling texture with the C-orientation dominant up to 97% reduction. The B-orientation increases only slightly up to 75%, but strongly at higher deformations and at 97% it even forms the texture maximum.

The cross rolled sample (Fig.1a,2a) depicts a very sharp, centrosymmetric texture with a pronounced  $\alpha$ -fibre (running at  $\varphi_2=0^\circ$ ,  $\phi=45^\circ$ , Fig.2b). Fig.3b shows the orientation densities along this  $\alpha$ -fibre for various degrees of deformation. It reveals a maximum around the  $\varphi_1=45^\circ$ -position, which increases in height and sharpness with increasing deformation and at 97% is nearly symmetric forming a peak at  $\varphi_1=45^\circ$ , i.e. in the  $\langle 011 \rangle \langle 755 \rangle$ -orientation. This is close to the  $\langle 011 \rangle \langle 322 \rangle$ -position reported earlier<sup>7-9</sup>.

## DISCUSSION OF THE DEFORMATION BEHAVIOUR

Straight Rolling: As  $\delta'$  precipitates very fast even at room temperature, it is not possible to completely suppress the  $\delta'$  precipitation<sup>10</sup>. Nevertheless, since the samples are cold rolled immediately after quenching, most of the alloyed Li is retained in solid solution. Consequently the deformation texture development is similar to that in other Al-alloys<sup>4-6</sup> leading to the observed strong C-orientation (Fig.2a, 3a). This is in accordance to Taylor type deformation models with a relaxed  $\epsilon_{NR}$ - and probably  $\epsilon_{NT}$ -shear<sup>4</sup>.

However, the strong increase of the B-orientation obtained with increasing deformation (Fig.2a,3a) cannot be explained by means of Taylor FC- or RC-models, if, as is mostly assumed for polycrystals, the  $\epsilon_{RT}$ -shear is constrained<sup>4</sup>. Due to the small amount of precipitated shearable  $\delta'$ -particles, the deformation mode tends to become localized<sup>11</sup>. But also Li-atoms in solid solution can probably cause planar slip due to recovery retardation<sup>12</sup> or short range order effects<sup>13</sup>. As can be seen metallographically (Fig.4), this gives rise to the formation of shear bands. Though not satisfactorily understood, these shear bands are assumed to ensue the strong increase of the G- and particularly of the B-orientation at high deformation levels, as discussed in<sup>5,6,12,14</sup>.

Cross Rolling does not reduce texture sharpness as sometimes assumed, but leads to a strong peak at  $\langle 011 \rangle \langle 755 \rangle$  as will now be discussed: After changing the rolling direction most orientations become unstable with regard to the new rolling coordinate system, and therefore no orientations as C and S which are stable during straight rolling can be formed. The  $B_1$ -orientation, however, is only  $20^\circ$  away from the  $B_2$ -orientation in the changed rolling coordinate system (Fig.5a) and  $\langle 011 \rangle \langle 755 \rangle$  lies exactly in the middle between these. Thus the two B-orientations rotate back and forth around ND at every rolling step subsequently forming the final  $\langle 011 \rangle \langle 755 \rangle$ -orientation by superimposition.

This behaviour is also confirmed by model calculations. For that purpose the Taylor FC- and RC-model program was applied here for a starting texture with 936 randomly distributed orientations<sup>4</sup> with the modi-

fication, that after each 10% reduction the orientations were rotated 90° around ND. Some results of the corresponding ODFs are shown in Fig.5. The figure proves good coincidence between the experimental (Fig. 1b,3b) and the theoretical textures for the FC-model (Fig.5a) as well as for the RC-model with free  $\epsilon_{NR}$  (Fig.5b), with the exception, that the maximum in the theoretical textures is much sharper than in the experimental ones. But such an increase in sharpness also occurs for Taylor modeling of straight rolling<sup>4</sup>. Furthermore, a quite strong Cube is predicted theoretically, but occurs only weakly experimentally.

### RECRYSTALLIZATION

Both the straight and cross rolled samples were subjected to a recrystallization treatment. Fig.6a,b shows the {111}-pole figures after 90% reduction and subsequent annealing for 90s at 410°C and Fig.7a,b shows the corresponding ODFs.

The straight rolled material reveals a recrystallization texture consisting of a {001}<100>-Cube with RD-scatterings towards a quite strong G-orientation {011}<100> and a {123}<634>-R-orientation. With increasing rolling degree the ratio between Cube- and R shifts towards R and with increasing annealing temperature towards Cube<sup>14</sup>. This texture is typical for Al, but, compared to pure Al<sup>15</sup> or e.g. Al-Mg-alloys<sup>12</sup>, very weak with the random part (phon) being ~30%.

Nucleation of recrystallization is assumed here to take place for the Cube in transition bands (according to the Dillamore/Kato-mechanism) and for the R-orientation at grain boundaries. Although both orientations have favourable growth conditions<sup>15</sup>, their final intensities are much less compared to pure Al. This is due to the Li-atoms in solid solution as well as to the finely dispersed  $\delta'$ -particles precipitated e.g. during recrystallization annealing. Both are known to reduce the growth preference of the Cube- and R-nuclei thus giving a better chance for growth of other, more randomly oriented nuclei<sup>6,14</sup>. This also leads to the very fine grained structure observed metallographically (Fig.8b).

Nucleation in shear bands, as described in other Al-alloys<sup>6,12</sup>, is only very rarely observed here (Fig.8a). This is due to the Li-depleted zones adjacent to the grain boundaries<sup>16</sup>: Nuclei formed here are less hindered by dissolved or precipitated Li, they obtain a growth advantage and finally also consume the shear bands. Nucleation in shear bands, however, probably causes the intensity of the G-orientation which is stronger than found in pure Al<sup>15</sup>. At very high deformations also other orientations being nucleated in shear bands are observed<sup>14</sup>.

The cross rolled samples exhibit a quite strong texture after recrystallization with four centro-symmetrical orientations. These orientations have a ~40° <111> orientation relationship to the B-orientations in the two rolling coordinate systems (Fig.6b) which by superimposition form the observed central {011}<755>-peak. Thus a good growth capacity into scatterings of the deformed structure is given. Furthermore the recrystallization orientations lay near to four S-orientations (two for each rolling coordinate system) of the deformed structure. Thus they are apparently able to act as nucleation sites.

## REFERENCES

1. O. Engler, J. Mizera, J. Driver, K. Lücke, this conference
2. J. Hirsch, O. Engler, K. Lücke, M. Peters, K. Welpmann, Proc. 4th Al-Li Conf., J. de physique, suppl. 9, Paris (1987) p.C3-605
3. O. Engler, K. Lücke, in press
4. J. Hirsch, K. Lücke, Acta metall. 36 (1988) p.2863/2883/2905
5. O. Engler, J. Hirsch, K. Lücke, Acta metall. 37 (1989) p.2743
6. K. Lücke, O. Engler, Mat. Sci. Tech. (1990) in press
7. R. Rixen, R. Musick, H. Göker, K. Lücke, Z. Metallk. 66 (1975) p.16
8. W.Y. Yeung, B.J. Duggan, Acta metall. 34 (1986) p.653
9. H. Hu, R.S. Cline, Textures and Microstructures 8,9 (1988) p.191
10. D.B. Williams, J.W. Edington, Metal Sci. 9 (1975) p.529
11. B. Noble, S.J. Harris, K. Dinsdale, Metal Sci. 16 (1982) p.425
12. P. Wagner, O. Engler, K. Lücke, this conference
13. V. Gerold, H.P. Karnthaler, Acta metall. 37 (1989) p.2177
14. F. Blasum, O. Engler, K. Lücke, to be published
15. J. Hirsch, Habilitation Thesis RWTH Aachen (1988)
16. P.L. Makin, W.M. Stobbs, Proc. 3rd Al-Li Conf., Oxford (1985) p.392

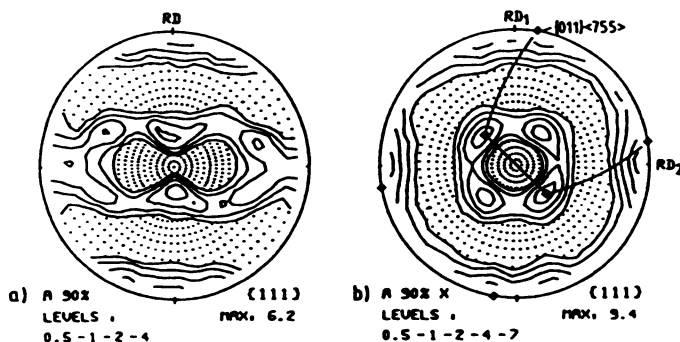


Fig.1:  $\{111\}$ -pole figures of the 90% a) straight rolled and b) cross rolled samples.

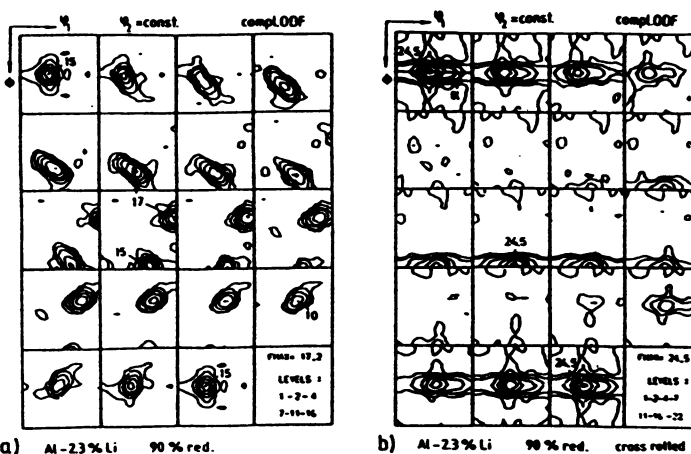


Fig.2: ODFs of the 90% a) straight rolled and b) cross rolled samples.

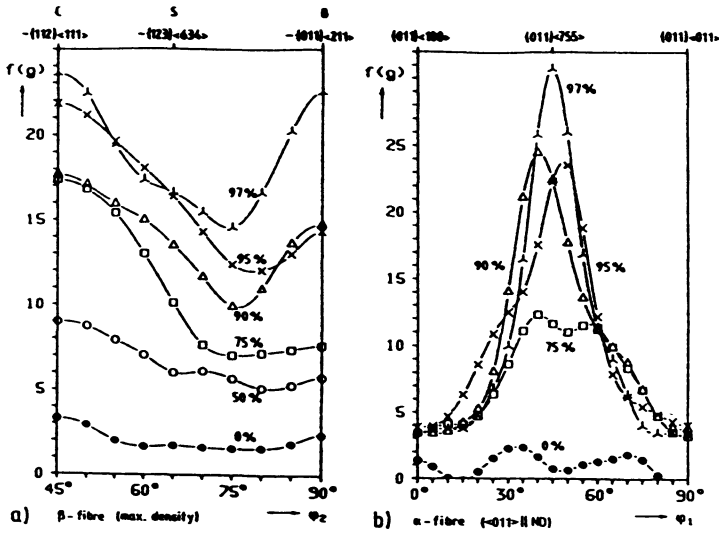


Fig. 3: a)  $\beta$ -fibres of the straight rolled and b)  $\alpha$ -fibres of the cross rolled samples. (Note different  $f(g)$ -scales!)

Fig. 4: Microstructure of the 90% straight rolled sample (anodically oxidated, longitudinal section 100x).

RD  $\rightarrow$  100  $\mu$ m

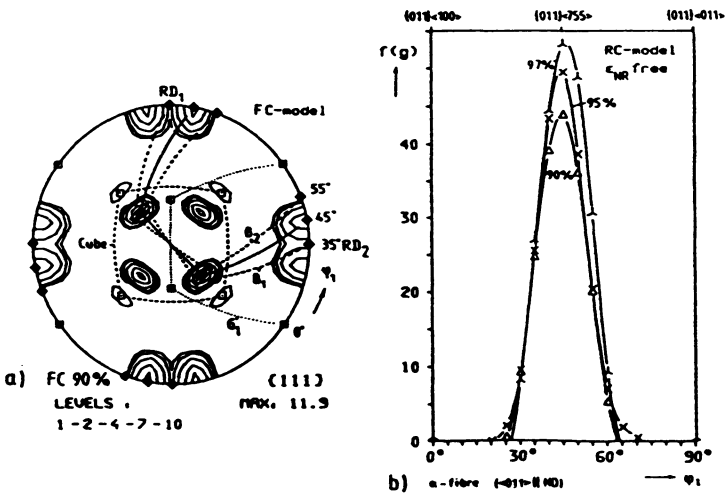
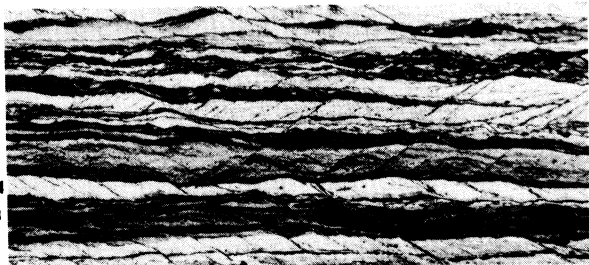


Fig. 5: a) recalculated  $\{111\}$ -pole figure and b)  $\alpha$ -fibres of the simulated cross rolling texture.

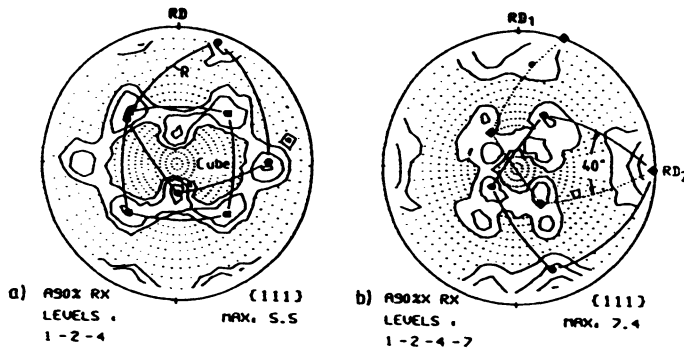


Fig. 6:  $\langle 111 \rangle$ -pole figures of the 90% a) straight rolled and b) cross rolled samples after recrystallization for 90s at 410°C.

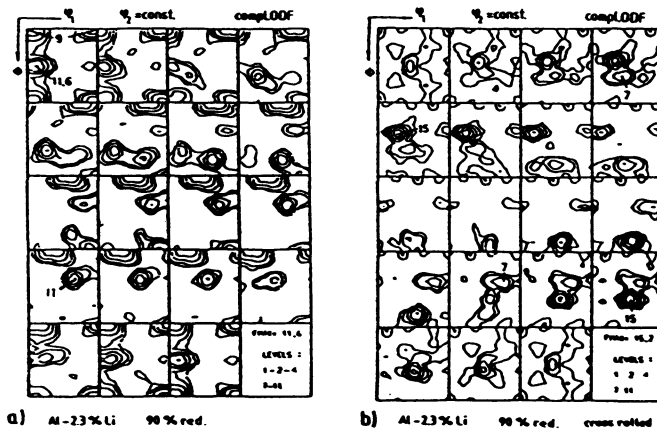


Fig. 7: ODFs of the 90% a) straight rolled and b) cross rolled samples after recrystallization for 90s at 410°C.

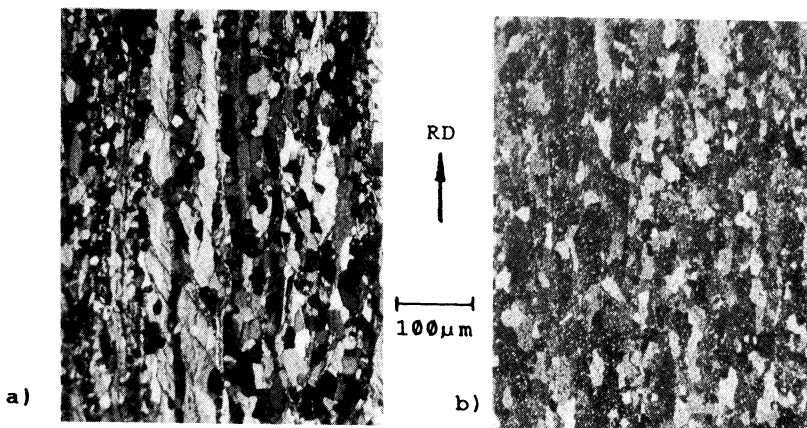


Fig. 8: Microstructure of the 90% straight rolled sample in the a) partially and b) completely recrystallized state (anodically oxidated, longitudinal section, 100 $\times$ ).